X-ray crystal-structure refinement of the nearly commensurate phase of $1T$-TaS_2 in $(3+2)$-dimensional superspace

Albert Spijkerman, Jan L. de Boer, Auke Meetsma, and Gerrit A. Wiegers
Department of Chemical Physics, Materials Science Center, University of Groningen, Nijenborgh 4, Nl-9747 AG Groningen, The Netherlands

Sander van Smaalen*
Laboratory of Crystallography, University of Bayreuth, D-95440 Bayreuth, Germany
(Received 2 December 1996; revised manuscript received 20 August 1997)

The structure of the nearly commensurate phase of $1T$-TaS_2 ($1T_2$-TaS_2) has been refined in $(3+2)$-dimensional superspace against single-crystal x-ray-diffraction data collected at 300 K. The intensities of main reflections and satellites up to sixth order were measured. The unique data set in $P\bar{3}$ consisted of 2652 observed reflections (233 main reflections, 1625 first- and second-order satellites and 794 higher-order satellites). For the refinement of the modulation amplitudes 21 harmonics on Ta and 12 harmonics on S were used. The structure agrees well with the discommensuration model proposed by Nakanishi and Shiba [J. Phys. Soc. Jpn. **43**, 1839 (1977)]. The structure determination by Yamamoto [Phys. Rev. B **27**, 7823 (1983)] is in agreement with the present one, within the limited resolution of Yamamoto's refinement. In each sandwich layer there are domains forming hexagons with a diameter of about 73 Å and within the center region 13-atom clusters of Ta atoms as present in the commensurate phase. It is shown that the domain structure in physical space directly corresponds to the modulation function displayed in additional space. [S0163-1829(97)07345-1]

I. INTRODUCTION

Tantalum disulfide belongs to the class of layered transition-metal dichalcogenides. These compounds are known for the possibility of charge-density-wave formation. Alternatively, variations of the structures exist due to polymorphism. The different structures are all based on a stacking of three-atom-thick layers, consisting of transition-metal atoms sandwiched between sulfur atoms.[1] Two types of layers have been found. Trigonal-prismatic layers have the transition-metal atom in a trigonal-prismatic coordination by S, and octahedral layers have a trigonal-antiprismatic (distorted octahedral) coordination. For TaS_2 the $2H$ polytype is stable at room temperature, and it is built of trigonal-prismatic layers only. The $1T$ modification consists solely of octahedral layers, and it is the stable modification above 850 °C. Also, polymorphs have been identified, in which both types of layers alternate, e.g., $6R$-TaS_2, $4H$(a)-TaS_2, $4H$(b)-TaS_2, $4H$(c)-TaS_2. Transitions between polymorphs were studied by van Landuy and co-workers[2] using electron diffraction.

Phase transitions in $1T$-TaS_2 express themselves by satellite reflections in electron diffraction,[3] and by an anomalous behavior of the temperature dependence of physical properties.[4] Above 850 °C the structure of $1T$-TaS_2 is of the $Cd(OH)_2$ type, with spacegroup $P\bar{3}m1$ and lattice parameters $a_0=b_0=3.36$ Å and $c_0=5.90$ Å (Fig. 1).[1] All phases below 850 °C can be described as a distortion of this basic structure.[2,5,6] It was found that well above 350 K the diffraction pattern is dominated by diffuse rings, which concentrate into spots on lowering the temperature. The positions of these diffuse spots can be described by an incommensurate wave vector $\mathbf{q}_I=0.283\mathbf{a}_0^*+\mathbf{c}_0^*/3$; this phase was called the $1T_1$-TaS_2 phase by Scruby and Williams,[5] and it was denoted as the incommensurate (IC) phase more recently. Below 350 K the wave vector rotates towards a position making an angle $\phi\approx 12°$ with $\mathbf{a}_0^*$ and becomes $\mathbf{q}_{\rm nc}=0.245\mathbf{a}_0^*+0.068\mathbf{b}_0^*+\mathbf{c}_0^*/3$ at $T=298$ K. This phase was called $1T_2$-TaS_2 by Scruby and Williams.[5] More recently, it was denoted the nearly commensurate (NC) phase, because the satellite reflections are close to the positions of superstructure reflections corresponding to a $\sqrt{13}a\times\sqrt{13}a\times 3c$ supercell. A first-order phase transition at 180 K results in the commensurate phase (C phase or $1T_3$-TaS_2), characterized by a $\sqrt{13}a\times\sqrt{13}a\times 13c$ supercell. The translation symmetry is characterized by in-plane basis vectors $\mathbf{a}=4\mathbf{a}_0+\mathbf{b}_0$ and $\mathbf{b}$

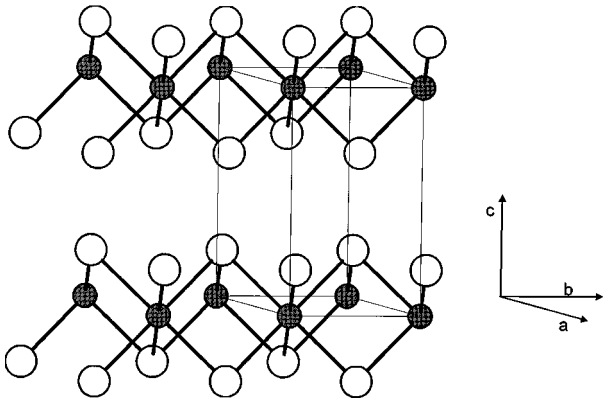

FIG. 1. The basic structure of $1T$-TaS_2. $1T$-TaS_2 is trigonal, spacegroup $P\bar{3}m1$, with lattice parameters $a_0=b_0=3.36$ Å and $c_0=5.90$ Å. One unit cell contains one Ta at (0,0,0) and two S at $\pm(\frac{1}{3},\frac{2}{3},z)$, $z\approx 0.25$ (Ref. 1). The Ta atoms are represented by filled circles.

$=-\mathbf{a}_0+3\mathbf{b}_0$. In reciprocal space, this corresponds to the commensurate wave vector $\mathbf{q}_c=(3\mathbf{a}_0^*+\mathbf{b}_0^*)/13=0.2308\mathbf{a}_0^*+0.0769\mathbf{b}_0^*$, and $\phi=13.9°$. The structure proposed for each of the layers in the C phase consists of hexagram-shaped clusters of 13 Ta atoms. The layers then would be stacked along the *c* axis with thirteen possibilities for the origin of each layer to be at one of the thirteen sites of the 13 cluster. Alternatively, Brouwer,[7] Fung and co-workers,[8] Tanda *et al.*,[9] and Nakanishi and Shiba[10] reported that the stacking is disordered, thus questioning the superperiod along **c**. On warming, the commensurate phase transforms into a triclinic phase (the T phase), with a stacking period of $7c_0$.

In this paper the structure is reported of $1T$-TaS_2 in its NC phase at room temperature. This phase is characterized by the occurrence of satellite reflections of many orders in the diffraction pattern,[15] contrary to the IC phase, where only a few low-order satellites can be found. Theoretically, the NC phase was studied by Nakanishi, Shiba, and co-workers[10,16,17] on basis of a Landau-Ginzburg expansion of the free energy. They found a discommensuration model comprised of domains with a commensurate structure as in the C phase, separated by discommensurations. Recently, the domain structure has been observed on the crystal surface by scanning tunnelling microscopy (STM) studies.[18–23]

Single-crystal x-ray data of the NC phase at 300 K were measured by Brouwer and Jellinek.[7,24] They determined a structure model in the commensurate (supercell) approximation ($\mathbf{a}=4\mathbf{a}_0+\mathbf{b}_0$, $\mathbf{b}=-\mathbf{a}_0+3\mathbf{b}_0$, and $\mathbf{c}=3\mathbf{c}_0$). This data set was limited in the sense that only first- and second-order satellites were measured reliably; higher-order satellites were measured at wrong positions, due to the commensurate approximation in data collection. The proposed structure involves 13 clusters of Ta atoms, similar to the structure proposed for the C phase. The structure factors measured by Brouwer[7] were used by Yamamoto[25] for refinement of the incommensurate structure in superspace.

We have performed a measurement of the x-ray scattering of $1T$-TaS_2 at room temperature. Satellites have been measured up to high orders, resulting in a much more extended data set, as was obtained by Brouwer. Refinements were done using the superspace formalism, and the resulting structure is analyzed both in superspace and in physical space. The domain structure is revealed in great detail, and the results are correlated with the results of STM experiments,[23] and the model based on Landau theory calculations.[17]

II. EXPERIMENT

Heating a mixture of Bi, Ta, and S resulted in a product with crystals, some of which could be identified as $1T$-TaS_2. X-ray-diffraction experiments were performed on an Enraf Nonius CAD4 diffractometer with Mo-K_α radiation ($\lambda=0.710\,73$ Å), using a crystal of dimensions $0.09\times0.09\times0.01$ mm. Unit-cell dimensions were obtained from the setting angles of 18 main reflections in four different settings with θ in the range 27–28°. At room temperature the lattice was found to be trigonal with lattice parameters $a_0=b_0=3.3649(1)$ Å and $c_0=5.8971(2)$ Å. These cell parameters are within standard deviations equal to those found by Brouwer.[7]

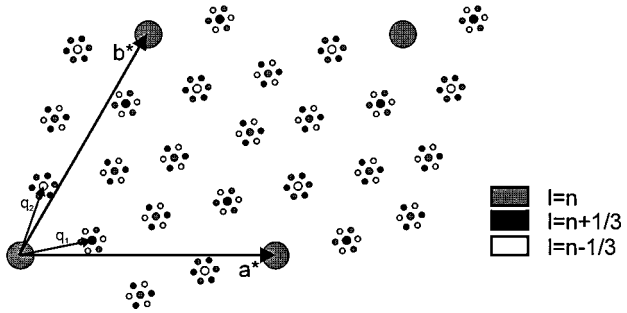

FIG. 2. Projection along **c*** of the reflection positions of $1T$-TaS_2 in the NC phase. The large spots are the main reflections and lie in planes $l_0=n$ ($n\in Z$). Each main reflection is surrounded by six first-order satellites lying in the planes $l_0=n+\frac{1}{3}$ and $l_0=n-\frac{1}{3}$ and by six second-order satellites lying in the plane $l_0=n$. Each first- or second-order satellite is surrounded by six higher-order satellites.

Satellite reflections could be indexed with five integers according to

$$\mathbf{S}=h\mathbf{a}_0^*+k\mathbf{b}_0^*+l\mathbf{c}^*+m_1\mathbf{q}^1+m_2\mathbf{q}^2, \tag{1}$$

where $\mathbf{c}^*=\mathbf{c}_0^*/3$. With respect to the reciprocal basis $\{\mathbf{a}_0^*,\mathbf{b}_0^*,\mathbf{c}^*\}$, the components of the modulation wave vectors are $\mathbf{q}^1=(\sigma_1,\sigma_2,0)$ and $\mathbf{q}^2=(-\sigma_2,\sigma_1+\sigma_2,0)$. From the positions of 161 satellite reflections the values $\sigma_1=0.2448(2)$ and $\sigma_2=0.0681(2)$ were obtained. Alternatively, the reflections can be indexed with respect to $\{\mathbf{a}_0^*,\mathbf{b}_0^*,\mathbf{c}_0^*\}$, but then the modulation wave vectors obtain commensurate components of $\pm\frac{1}{3}$ along $\mathbf{c}_0^*$. Using l_0 as the index corresponding to $\mathbf{c}_0^*$, first-order satellites are found in the planes $l_0=n\pm\frac{1}{3}$ ($n\in Z$). Each main reflection is surrounded by six first-order satellites, which have the indices (h,k,l,m_1,m_2) with (m_1,m_2) equal to $\pm(1,0)$, $\pm(0,1)$, and $\pm(1,-1)$, respectively, (Fig. 2). Second-order satellites of the type (1,1) are present in the planes $l_0=n$. Because the components of the modulation wave vectors along a_0^* and b_0^* are large, higher-order satellites are far from the main reflections with the same indices h, k, and l. However, higher-order satellites are found close to the lower-order satellites, which are formally assigned to other main reflections. For example, satellites $(h,k,l,m_1,m_2)=(h,k,l,1,2)$ are close to the first-order satellites $(h,k+1,l-1,0,-1)$ (Fig. 2). In total, each first- and second-order satellite is surrounded by six satellites of the next-higher orders, resulting in 84 satellites corresponding to each main reflection. The assignment of reflections to groups of a particular satellite order is not straightforward. A physically meaningful classification should give the same order to symmetry equivalent reflections. Because the modulation wave vectors are related by the threefold axis, this implies that ''order of a satellite'' cannot be represented by a single number anymore. Taking into account symmetry, reflections (h,k,l,m_1,m_2) can be divided into the following fifteen groups defining the same order, with (m_1,m_2) is equal to (0,0); (1,0)(0,1)(−1,1); (1,1)(−1,2)(−2,1); (2,0)(0,2)(−2,2); (1,2)(−2,3)(−3,1); (2,1)(−1,3)(−3,2); (3,0)(0,3)(−3,3); (4,0)(0,4)(−4,4); (5,0)(0,5)(−5,5); (2,2)(−2,4)(−4,2); (2,4)(−4,6)(−6,2); (3,1)(−1,4)(−4,3); (3,2)(−2,5)(−5,3); (1,4)(−4,5)

TABLE I. Symmetry restrictions on the parameters of the modulation functions in the NC phase of $1T$-TaS_2 [Eq. (4)].

Ta at (0,0,0)	S at $\pm(\frac{1}{3},\frac{2}{3},z)$
$A^x_{-m_1-m_2,m_1}=-A^x_{m_1,m_2}+A^x_{-m_2,m_1+m_2}$	$A^x_{-m_1-m_2,m_1}=-A^x_{m_1,m_2}+A^x_{-m_2,m_1+m_2}$
$A^y_{m_1,m_2}=A^x_{m_1,m_2}-A^x_{-m_2,m_1+m_2}$	$A^y_{m_1,m_2}=A^x_{m_1,m_2}-A^x_{-m_2,m_1+m_2}$
$A^y_{-m_2,m_1+m_2}=A^x_{m_1,m_2}$	$A^y_{-m_2,m_1+m_2}=A^x_{m_1,m_2}$
$A^y_{-m_1-m_2,m_1}=A^x_{-m_2,m_1+m_2}$	$A^y_{-m_1-m_2,m_1}=A^x_{-m_2,m_1+m_2}$
$A^z_{m_1,m_2}=-A^z_{-m_2,m_1+m_2}=A^z_{-m_1-m_2,m_1}$	$A^z_{m_1,m_2}=-A^z_{-m_2,m_1+m_2}=A^z_{-m_1-m_2,m_1}$
$B^x_{m_1,m_2}=B^x_{-m_2,m_1+m_2}=B^x_{-m_1-m_2,m_1}=0$	$B^x_{-m_1-m_2,m_1}=-(B^x_{m_1,m_2}+B^x_{-m_2,m_1+m_2})$
$B^y_{m_1,m_2}=B^y_{-m_2m_1+m_2}=B^y_{-m_1-m_1-m_2,m_1}=0$	$B^y_{m_1,m_2}=B^x_{m_1,m_2}+B^x_{-m_2,m_1+m_2}$
$B^z_{m_1,m_2}=B^z_{-m_2,m_1+m_2}=B^z_{-m_1-m_2,m_1}=0$	$B^y_{-m_2,m_1+m_2}=-B^x_{m_1,m_2}$
	$B^y_{-m_1-m_2,m_1}=-B^x_{-m_2,m_1+m_2}$
	$B^z_{m_1,m_2}=B^z_{-m_2,m_1+m_2}=B^z_{-m_1-m_2,m_1}$

$(-5,1)$; $(2,3)(-3,5)(-5,2)$. Furthermore, the reflections with both m_1 and m_2 with opposite sign belong to the reflection groups also.

The integrated intensities up to scattering angle $\theta=40°$ were measured for the main reflections and all of the above mentioned 84 satellites assigned to each main reflection. From this dataset 1, the reflections were selected with intensities larger than two times their standard deviation, and they were remeasured with a longer counting time (320 s), resulting in dataset 2. Corrections to the measured counts were applied for to variation of the intensity control reflection (maximum correction 3.53%), absorption ($\mu^{TaS_2}=487.0\ cm^{-1}$, resulting in minimum/maximum transmission factors of 0.118 and 0.613, respectively), and Lorentz and polarization factors. Dataset 2 contained 3464 reflections that reduced to 3069 unique reflections using Laue symmetry 3, with an internal consistency of 0.08. Using the criterion for observed reflections $I>2\sigma(I)$, the reduced dataset 2 comprised of 233 observed main reflections, 1625 observed first- and second-order satellites, 794 observed higher-order satellites, and 417 less than's. The observed data were used in the structure refinement. The final structure model was also tested against the less than's in dataset 1.

III. SYMMETRY AND REFINEMENT

The spacegroup of the basic structure of $1T_2$-TaS_2 is $P\bar{3}m1$.[7] Including satellite reflections, the diffraction pattern is found to be compatible with the $(3+2)$-dimensional superspace group $P\bar{3}(\alpha,\beta,\frac{1}{3})$,[26] which was confirmed as the superspace symmetry of the structure by the subsequent refinements. The complete analysis has been done with a basic structure unit cell containing the tripled $\bar{c}$-axis [Eq. (1)]. Then the commensurate components are removed from the modulation wave vectors, and the structure has the centering translations $(E|0,0,\frac{1}{3},\frac{2}{3},\frac{1}{3})$ and $(E|0,0,\frac{2}{3},\frac{1}{3},\frac{2}{3})$. The superspace symmetry is characterized by the 3 operator $(x_2,-x_1+x_2,-x_3,x_5,-x_4+x_5)$.

The positions of the atoms in the modulated structure are given as the sum of a translational symmetric basic structure position $\bar{\mathbf{r}}=(\bar{x_1},\bar{x_2},\bar{x_3})$, and the value of a modulation function $\mathbf{u}(\bar{x_4},\bar{x_5})$, evaluated at the basic structure position:

$$\mathbf{r}^\mu(\bar{x_4},\bar{x_5})=\bar{\mathbf{r}^\mu}+\mathbf{u}^\mu(\bar{x_4},\bar{x_5}). \tag{2}$$

The modulation functions are periodic with periods one in their arguments, with the latter defined as

$$\bar{x_4}=\mathbf{q}^1\cdot\bar{\mathbf{r}}+t_1,$$
$$\bar{x_5}=\mathbf{q}^2\cdot\bar{\mathbf{r}}+t_2. \tag{3}$$

Due to the incommensurability of the modulation, the starting phases of the modulation, t_1 and t_2, can be assigned arbitrary values. The modulation functions are written as a Fourier series:

$$u^\mu_\alpha(\bar{x_4},\bar{x_5})=\sum_{n_1=0}^{\infty}\sum_{n_2=0}^{\infty}A^\mu_{n_1n_2\alpha}\sin(2\pi n_1\bar{x_4}+2\pi n_2\bar{x_5}) + B^\mu_{n_1n_2\alpha}\cos(2\pi n_1\bar{x_4}+2\pi n_2\bar{x_5}), \tag{4}$$

where $\alpha=1,2,3$, μ indicates the atom, (n_1,n_2) defines the order of the harmonic, and the term (0,0) is excluded from the summation. Three coordinates characterizing the basic structure position, the amplitudes $A^\mu_{n_1n_2\alpha}$ and $B^\mu_{n_1n_2\alpha}$, and the temperature parameters are the independent parameters for atom μ used in the refinement.

The basic structure of $1T$-TaS_2 contains two independent atoms, with Ta on the special position (0,0,0), and with S on $(\frac{1}{3},\frac{2}{3},z)$, corresponding to site symmetries 3 and 3, respectively. The modulation functions of these atoms have to adhere to this site symmetry also.[27] Because of the threefold symmetry, the amplitudes of different orders (m_1,m_2) segregate into groups of related amplitudes, in the same way as the different satellites were assigned to a group of the same order (Sec. II). The resulting symmetry restrictions on the parameters of the modulation functions [Eq. (4)] for site symmetry 3 (valid for the Ta atom) and for site symmetry 3 (valid for S) are summarized in Table I.

IV. DETERMINATION OF THE STRUCTURE

Refinements were performed using the program JANA94.[28] The site symmetry implies that harmonics have to be included into the modulation function in groups of six symmetry related parameters describing the x and y displacements, and three symmetry related parameters for the z displacements. They correspond to two independent parameters and one independent parameter, respectively, (Table I). Further-

TABLE II. Partial R factors and number of reflections for the different reflection orders used in the refinement of $1T$-TaS_2. The reflection groups are defined by the (m_1,m_2) indices of the reflections (see text).

Reflection group (m_1,m_2)	No. observed reflections	R_F	wR_F^2
Main=(0,0)	233	0.038	0.053
(1,0)(0,1)(−1,1)	1045	0.064	0.078
(1,1)(−1,2)(−2,1)	580	0.068	0.068
(2,0)(0,2)(−2,2)	323	0.153	0.139
(1,2)(−2,3)(−3,1)	232	0.141	0.129
(2,1)(−1,3)(−3,2)	62	0.423	0.466
(3,0)(0,3)(−3,3)	51	0.411	0.495
(4,0)(0,4)(−4,4)	17	0.515	0.666
All	2543	0.071	0.081

more, for the Ta atom all cosine parameters are zero.

The starting models for the modulated structure involved basic structure parameters as determined from the refinement on the main reflections only. With the initial values of all modulation parameters equal to zero, the refinement converged to a bad fit. A starting model with values assigned to the six lowest-order harmonics of the modulation function of Ta, in accordance with model of Brouwer,[7] resulted in a good fit after refinement (Table II).

The structure model was varied by subsequently introducing more harmonics into the refinement. The best fit was obtained with 21 harmonics for the Ta atom, corresponding to 21 independent modulation parameters, and 12 harmonics for the S atom, corresponding to 24 independent parameters. The introduction of more harmonics for the modulation of S lead to parameters with high standard deviations and negative temperature factors. The introduction of more harmonics for the modulation of Ta resulted in amplitudes of these harmonics of the order of their standard deviations, while the R factors did not improve. The higher-order satellites are not fitted well (Table II), but we found that the presence of these satellites in the reflection list improved the stability of the fit. Still higher-order harmonics in the modulation functions are required to obtain a better description of the intensities of these satellite orders, but, apparently, the small number of observed reflections among these groups of satellites does not allow to determine the values of the corresponding harmonics of the modulation functions. The structural parameters for the NC phase of $1T$-TaS_2 are presented in Tables III, IV, and V.

TABLE III. Parameters of the average structure of $1T$-TaS_2 after refinement with 21 harmonics for Ta and 12 harmonics for S. The parameters refer to the $a_0\times a_0\times 3c_0$ cell. The x, y, and z are fractional coordinates. Temperature parameters U_{ij} are in $Å^2$. $U_{13}=U_{23}=0$ by symmetry. $U_{22}=U_{11}=2U_{12}$.

Atom	x	y	z	U_{11}	U_{33}
Ta	0	0	0	0.0061(1)	0.0069(2)
S	$\frac{1}{3}$	$\frac{1}{3}$	0.0862(1)	0.0071(4)	0.0086(7)

TABLE IV. Modulation parameters for the Ta atom after refinement of $1T$-TaS_2. The atomic displacement for the Ta atom is given by Eq. (4). The parameters are given in angstrom and refer to the $a_0\times a_0\times 3c_0$ cell. Parameters without standard deviation are dependent on other parameters (see Table I). The amplitudes B_{n_1,n_2} are all zero by symmetry.

n_1,n_2	$A^x_{n_1,n_2}$	$A^y_{n_1,n_2}$	$A^z_{n_1,n_2}$
1,0	−0.1362 (2)	−0.0676	0.0043
0,1	−0.0685 (1)	−0.1362	−0.0043
−1,1	0.0676	−0.0685	0.0043 (0)
1,1	0.0571 (3)	−0.0053	−0.0008
−1,2	0.0624 (3)	0.0571	0.0008
−2,1	0.0053	0.0624	−0.0008 (4)
2,0	0.0122 (4)	0.0461	0.0024
0,2	−0.0339 (4)	0.0122	−0.0024
−2,2	−0.0461	−0.0339	0.0024 (5)
1,2	0.0000 (8)	0.0281	−0.0028
−2,3	−0.0280 (7)	0.0000	0.0028
−3,1	−0.0281	−0.0280	−0.0028 (8)
2,1	−0.0231 (7)	−0.0217	0.0011
−1,3	−0.0014 (7)	−0.0231	−0.0011
−3,2	0.0217	−0.0014	0.0011 (12)
3,0	−0.0221 (12)	−0.0387	−0.0018
0,3	0.0165 (11)	−0.0221	0.0018
−3,3	0.0387	0.0165	−0.0018 (12)
4,0	0.0399 (21)	0.0371	0.0144
0,4	0.0028 (21)	0.0399	−0.0144
−4,4	−0.0371	0.0028	0.0144 (25)

V. DISCUSSION

A domain structure with infinitely sharp domain walls can be described by a block-wave modulation of the underlying basic structure. The present refinement showed that a large number of terms in the Fourier expansions of the modulation functions were nonzero, indicating a strong deviation from harmonicity, prerequisite for the modulation function to be block-wave like. It will be shown below that the concept of domains with a commensurate $\sqrt{13}a\times\sqrt{13}a$ superstructure, and separated by domain walls, is indeed found in the present structure determination. Size and shape of the domains and some information about the domain walls is obtained.

A. Clusters of Ta atoms

The modulation of the Ta atom is found to be mainly in the **a**, **b** plane (Table IV). The modulation functions can be analyzed by displaying their values as a function of t_1 and t_2 [Eqs. (2)–(4)].[27] Instead of tabulating the values of the modulation functions in the different unit cells [varying $\overline{\mathbf{r}}$ in Eq. (2)], t_1 and t_2 can be varied continuously. Because the modulation is periodic, all its values occurring anywhere in the structure thus are contained in this t plot for $0<t_1<1$ and $0<t_2<1$. In addition to the values of modulation function, their magnitudes, interatomic distances, and other parameters can be displayed as a function of t_1 and t_2. As an example consider the distance between Ta (0,0,0) and Ta (1,0,0) (Fig. 3). The Ta atom on (0,0,0) has $\mathbf{q}^1\cdot\overline{\mathbf{r}}=0$ and

TABLE V. Modulation parameters for the S atom after refinement of $1T$-TaS_2. The atomic displacement for the S atom is given by Eq. (4). The parameters are given in angstrom and refer to the $a_0 \times a_0 \times 3c_0$ cell. Parameters without standard deviation are dependent on other parameters (see Table I).

n_1,n_2	$A^x_{n_1,n_2}$	$A^y_{n_1,n_2}$	$A^z_{n_1,n_2}$	$B^x_{n_1,n_2}$	$B^y_{n_1,n_2}$	$B^z_{n_1,n_2}$
1,0	−0.0243 (10)	−0.0100	0.0189	−0.0085 (9)	0.0022	−0.0520
0,1	−0.0142 (7)	−0.0243	−0.0189	0.0107 (6)	0.0085	−0.0520
−1,1	0.0100	−0.0142	0.0189 (10)	−0.0022	0.0107	−0.0520 (8)
1,1	0.0041 (11)	−0.0048	−0.0159	0.0109 (11)	0.0042	0.0066
−1,2	0.0089 (10)	0.0041	0.0159	−0.0067 (10)	−0.0109	0.0066
−2,1	0.0048	0.0089	−0.0159 (15)	−0.0042	0.0067	0.0066 (14)
2,0	−0.0047 (19)	−0.0005	0.0046	−0.0034 (20)	−0.0103	0.0048
0,2	−0.0042 (15)	−0.0047	−0.0046	−0.0069 (16)	0.0034	0.0048
−2,2	0.0005	−0.0042	0.0046 (20)	0.0103	0.0069	0.0048 (21)
1,2	−0.0003 (30)	−0.0037	0.0091	−0.0004 (30)	0.0028	0.0054
−2,3	0.0034 (22)	−0.0003	−0.0091	0.0032 (21)	0.0004	0.0054
−3,1	0.0037	0.0034	0.0091 (30)	−0.0028	−0.0032	0.0054 (29)

$\mathbf{q}^2 \cdot \overline{\mathbf{r}} = 0$, while the Ta atom on (1,0,0) has $\mathbf{q}^1 \cdot \overline{\mathbf{r}} = 0.245$ and $\mathbf{q}^2 \cdot \overline{\mathbf{r}} = -0.068$ [Eq. (3)]. The distance between these atoms is displayed in the t plot at the point $t_1 = 0$ and $t_2 = 0$ (Fig. 3). The distance between neighbors Ta (n_1,n_2,n_3) and Ta $(1+n_1,n_2,n_3)$ can be computed by substituting (n_1,n_2,n_3) and $(1+n_1,n_2,n_3)$ for $\overline{\mathbf{r}}$ [Eqs. (2)–(4)]. Alternatively, this distance can be read off Fig. 3 at the point $(t_1,t_2) = (\mathbf{q}^1 \cdot \mathbf{n} \pmod 1,\ \mathbf{q}^2 \cdot \mathbf{n} \pmod 1)$.

A useful property of the t plots is that different functions can be compared directly, in order to study the local structure as a function of (t_1,t_2), i.e., as a function of the position in the crystal. For example, the distance between Ta (0,0,0) and Ta (1,0,0) (Fig. 3) can be compared with the distance between Ta (0,0,0) and Ta (0,1,0) (Fig. 4). These plots are equivalent, apart from a rotation to be applied to the coordinate axis (Fig. 4 is obtained from Fig. 3 by the transformation: $t_1' = -t_2$, $t_2' = t_1 - t_2$). However, retaining both representations of the Ta neighbor distances directly shows part of the coordination of Ta (0,0,0) by its neighbor's Ta (1,0,0) and Ta (0,1,0), as the values at $t_1 = t_2 = 0$ in the two plots, respectively. The coordination of Ta (n_1,n_2,n_3) by Ta (1

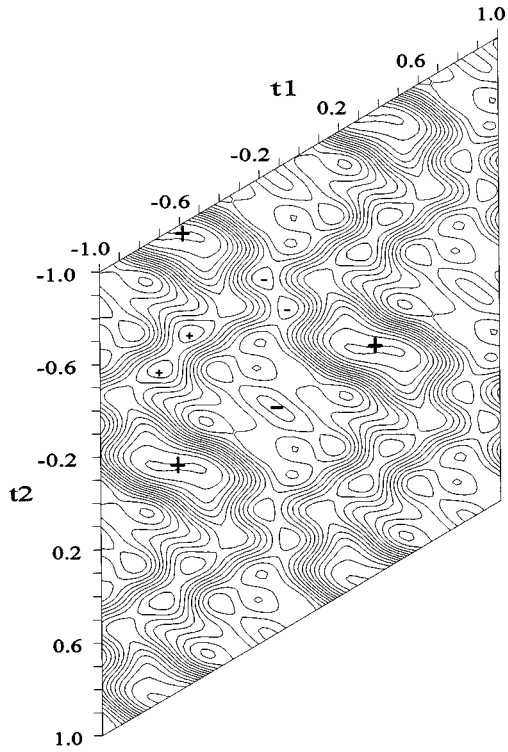

FIG. 3. Distance between Ta (0,0,0) and Ta (1,0,0) as a function of (t_1,t_2) [Eqs. (2)–(4)]. Contours of constant distance are drawn at intervals of 0.05 Å. The larger minus sign indicates the absolute minimum (3.086 Å) and the larger plus sign the absolute maximum (3.806 Å) in the plot. The smaller plus and minus signs indicate local maxima and minima.

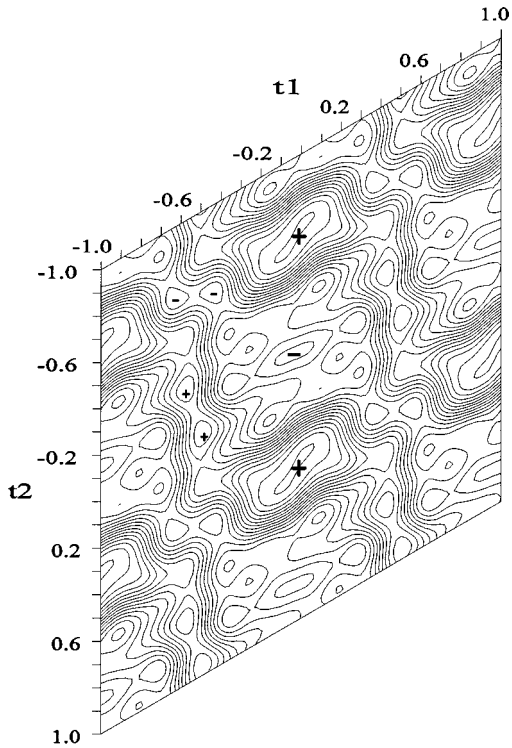

FIG. 4. Distance between Ta (0,0,0) and Ta (0,1,0). The contour interval is 0.05 Å. The larger minus sign indicates the shortest distance (3.086 Å) and the larger plus sign the longest distance (3.806 Å). The smaller plus and minus signs indicate local maxima and minima.

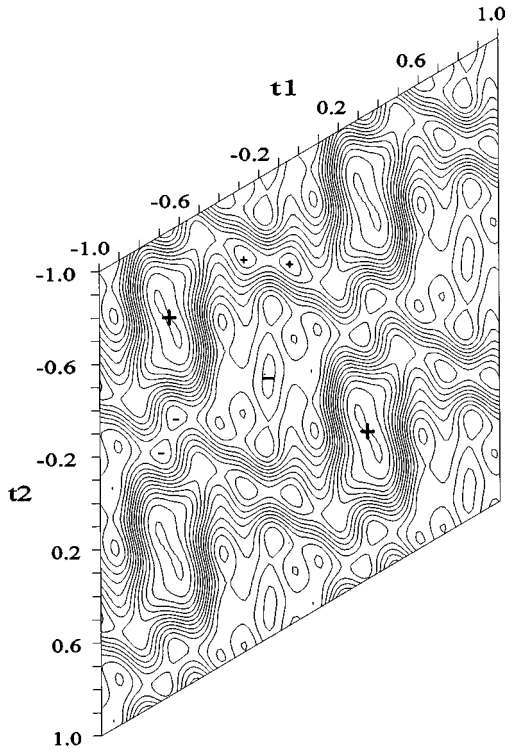

FIG. 5. Distance between Ta (0,0,0) and Ta (1,1,0). The contour interval is 0.05 Å. The larger minus sign indicates the shortest distance (3.086 Å) and the larger plus sign the longest distance (3.806 Å). The smaller plus and minus signs indicate local maxima and minima.

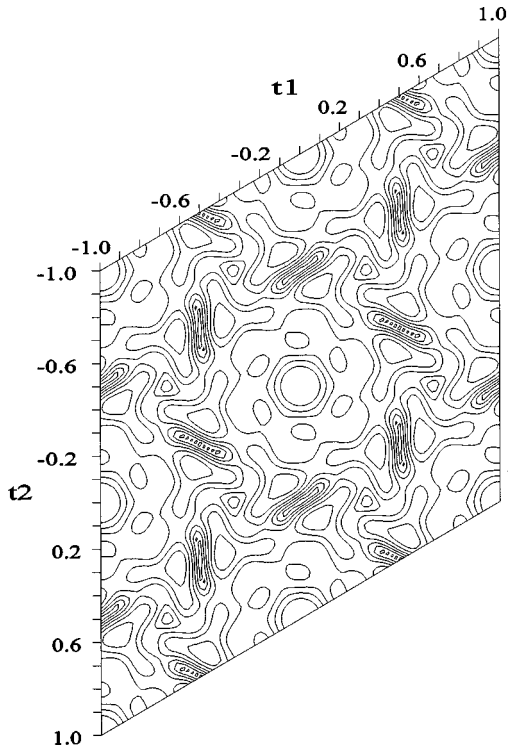

FIG. 6. Magnitude of the x,y displacement of the modulated Ta atom. The contour interval is 0.044 Å. The minimum is of 0.0 Å is found at $(t_1,t_2)=(0.0,0.0)$, (0.0,0.5), (0.5,0.0), and (0.5,0.5). The maximum is 0.308 Å.

$+n_1,n_2,n_3)$ and Ta $(n_1,1+n_2,n_3)$, then follow from Figs. 3 and 4 at the points $(t_1,t_2)=(\mathbf{q}^1\cdot\mathbf{n} \pmod 1,\ \mathbf{q}^2\cdot\mathbf{n} \pmod 1)$. Thus, the two figures together display the variation throughout the structure of part of the local configuration around the Ta atom.

These properties can be used to show the formation of 13 clusters by analyzing t plots. Figure 3 shows that the distance between neighboring atoms Ta (n_1,n_2,n_3) and Ta $(1+n_1,n_2,n_3)$ has a global minimum at $(t_1,t_2)=(0,0)$ corresponding to $n_1=n_2=n_3=0$. This point is at the center of a plateau of short interatomic distances, while at other values for the argument (t_1,t_2) larger than average distances are found (Fig. 3). The block-wave character of the modulation function thus shows up in the distance plot. In the basic structure each Ta atom has six nearest neighbors of this type, which are related by rotational symmetry. The formation of clusters of Ta atoms then requires that that all these six distances around a central atom Ta (n_1,n_2,n_3) simultaneously become shorter than average. As discussed above, Figs. 3 and 4 already compare two such distances. Superposition of the six t plots corresponding to all six distances around Ta (0,0,0) then shows that there is a common area in (t_1,t_2), centered on (0,0), where all distances become shorter than average (Figs. 3, 4, and 5). For values (n_1,n_2,n_3) corresponding to values (t_1,t_2) in this area, the atom Ta (n_1,n_2,n_3) has six nearest neighbors at shorter than average distances, and a cluster of seven atoms exists. Furthermore, superposition of these t plots and those of distances between Ta (0,0,0) and its next-nearest neighbors, then shows that there still is a common region where all these distances are less than average. This correlation then is the indication that 13 clusters of Ta atoms exist in the structure, in agreement with the results of Brouwer.[7] The diameter of this region is approximately 0.2 in either t_1 or t_2. The area of this common region is directly proportional to the fraction of Ta atoms that form the center atom of a 13 cluster. The fraction of atoms that are part of a 13 cluster thus is 13 times that area, and it follows that approximately a fraction of 13 times $(0.2)^2\approx 0.5$ of the Ta atoms is part of a 13 cluster. Consideration of still further neighbors, or, for example, of the distance between Ta (1,0,0) and Ta (2,0,0) shows that this distance is larger than average for those values of (t_1,t_2) for which the distance between Ta (0,0,0) and Ta (1,0,0) is smaller than average. The clusters thus are restricted to 13 atoms indeed.

The block-wave character of the modulation function of Ta is difficult to visualize directly, because x and y displacements are of equal importance. Instead of studying the components independently, the magnitude of the displacement in the x,y plane has been calculated (Fig. 6). Of course, this plot contains only positive values. Ta lies on the 3 axis, which for the two-dimensional $\overline{x_4},\overline{x_5}$ space implies six-fold symmetry of the modulation functions, and this symmetry is indeed seen in Fig. 6. Whereas the modulation functions should show the full site symmetry, distance functions between atoms may have a lower symmetry, as is obvious from the comparison with Fig. 3. Centered on the origin $(t_1=t_2=0)$, the x,y displacement exhibits a circular plateau of magnitude zero, representing the block-wave character of the modulation function. It implies that Ta atoms with phases

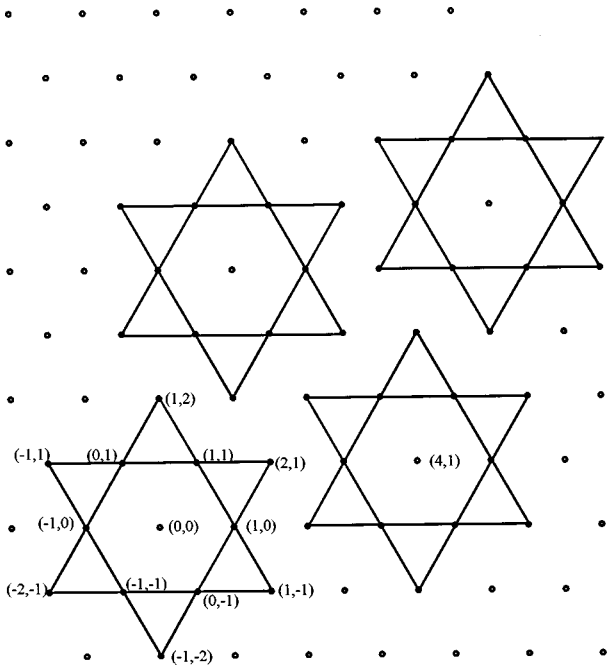

FIG. 7. One layer of Ta atoms of the average structure of $1T$-TaS_2, e.g., for $z \equiv 0$. Numbers refer to the x,y coordinates of the Ta atoms.

$(\overline{x_4},\overline{x_5})$ in the neighborhood of (0,0) are not shifted from their average position, again an indication that these Ta atoms are the central atoms of the 13 clusters. Furthermore elongated valleys are present, which also refer to regions, where the displacement is close to zero. As shown below, atoms with $(\overline{x_4},\overline{x_5})$ in these regions form the atoms of the domain walls.

B. The domain structure

The commensurate phase has a $\sqrt{13}a \times \sqrt{13}a$ superstructure, and its unit cell contains precisely one 13 cluster of Ta atoms. The centers of these clusters again form a trigonal lattice (Fig. 7). With respect to the small, basic structure unit cell, the atoms forming the centers of the 13 clusters are given by $(n_1,n_2,n_3)=(4n,n,n_3)$ and equivalents by rotation symmetry, for Ta $(0,0,n_3)$ being at the center of a 13 cluster. With the commensurate modulation wave vectors $\mathbf{q}_c^1=(3\mathbf{a}_0^*+\mathbf{b}_0^*)/13$ and $\mathbf{q}_c^2=(\mathbf{a}_0^*-4\mathbf{b}_0^*)/13$, the arguments of the modulation functions of these atoms follow as $(\overline{x_4},\overline{x_5})=(n,0)$. Going from cluster n to cluster $n+1$ changes the phase of the modulation by (1,0) and the modulation amplitude remains the same. For the NC structure, the difference of the phase of the modulation between the atoms Ta (n_1,n_2,n_3) and Ta (n_1+4,n_2+1,n_3) is $(1+\delta\overline{x_4},\delta\overline{x_5})=(1.047,0.041)=[0.047\ (\mathrm{mod}\ 1),0.041\ (\mathrm{mod}\ 1)]$. It was shown above, that the atoms that form the centers of 13 clusters approximately lie within a circle of radius 0.1 around the origin in $(\overline{x_4},\overline{x_5})$ space. From the value for $(\delta\overline{x_4},\delta\overline{x_5})$ between atoms a translation (4,1,0) apart, it follows that in any direction a maximum of five consecutive 13 clusters can be found, after which the sequence interrupted. That implies a structure consisting of domains of diameter of approximately five 13 clusters, and each domain has a structure similar to that of the commensurate $\sqrt{13}a \times \sqrt{13}a$ superstructure.

Within the first domain, the centers of the 13 clusters are at the atoms Ta $(4n,n,0)$. For $n=7$, it is not Ta $(4n,n,0)$ but it is Ta $(4n-1,n-1,0)$ that has $[\overline{x_4}\ (\mathrm{mod}\ 1),\ \overline{x_5}\ (\mathrm{mod}\ 1)]$ approximately equal to (0,0), and it are these atoms which will be the centers of the 13 clusters in the next domain. The domain wall is found to comprise a missing row of atoms, and the structure determination thus reveals the nature of the discommensurations to be in agreement with theory.[17,29] However, the incommensurateness requires that the nature of the discommensuration must vary. It can be derived that in the direction $(4n,n,0)$ occasionally the domain wall corresponds to an additional row of atoms corresponding to the center of the clusters shifting from Ta $(4n,n,0)$ towards Ta $(4n,n-1,0)$, in agreement with STM studies.[23]

The positions of the atoms in physical space can be calculated directly from the modulation functions and basic-structure coordinates. This has been done for the layers of Ta atoms at $z=0$ [Fig. 8(a)] and at $z=\frac{1}{3}$ [Fig. 8(b)] for an area of 100×100 unit cells. Only the Ta atoms belonging to a complete 13 cluster have been plotted, where a complete cluster is defined in the following way. The average distance between a central atom and any of its six nearest-neighbor Ta atoms is 3.36 Å and the distance towards the next-nearest neighbors is 5.81 Å (Fig. 7). A 13 cluster is defined as a cluster on a central Ta atom, if its six nearest neighbors have distances less than 3.36 Å, and if its six next-nearest neighbors have distances less than 5.85 Å. The sizes and shapes of the domains are obvious in these plots, and they have a diameter of about five 13 clusters, as was also derived directly from the t plots. Alternatively, the average domain size can be calculated from the difference between the incommensurate modulation wave vector and its commensurate approximation valid within the domains.[16,22] For the present values of $\mathbf{q}^1$ and $\mathbf{q}^2$, a diameter is found of 73 Å, in agreement with the center-to-center distances in Fig. 8. Additional information carried by the modulation functions pertains to the shapes of the domains and the thicknesses and shapes of the domain walls. Due to the incommensurateness of the modulation with the lattice of atoms carrying the displacement wave, different domains must have differences in their structures, size, or shape, and this is indeed found in Fig. 8.

The modulation function of Ta indicates almost zero displacement for values of (t_1,t_2) in elongated valleys (Fig. 6). Comparison of Fig. 6 with Figs. 3, 4, and 5 shows that Ta atoms with $(\overline{x_4},\overline{x_5})$ in these regions never belong to a 13 cluster, and therefore that they are in the domain walls. In physical space, these atoms are found as the isolated lying dots in the domain wall region [Fig. 8(c)], and it follows that in the domain walls there are more distances longer than average, contrary to the structure within the domains, which shows more distances shorter than average. Because, the elongated valleys make angles of 60° with each other, domain walls exist, which make angles of 60° and 120° also, and the shape of the domains can be approximated by a hexagon. Most notably, these hexagons do not form a honeycomb lattice, but instead, our result is better described by hexagon-shaped domains sharing vertices (Fig. 9). The domain-wall region can then be characterized as a network

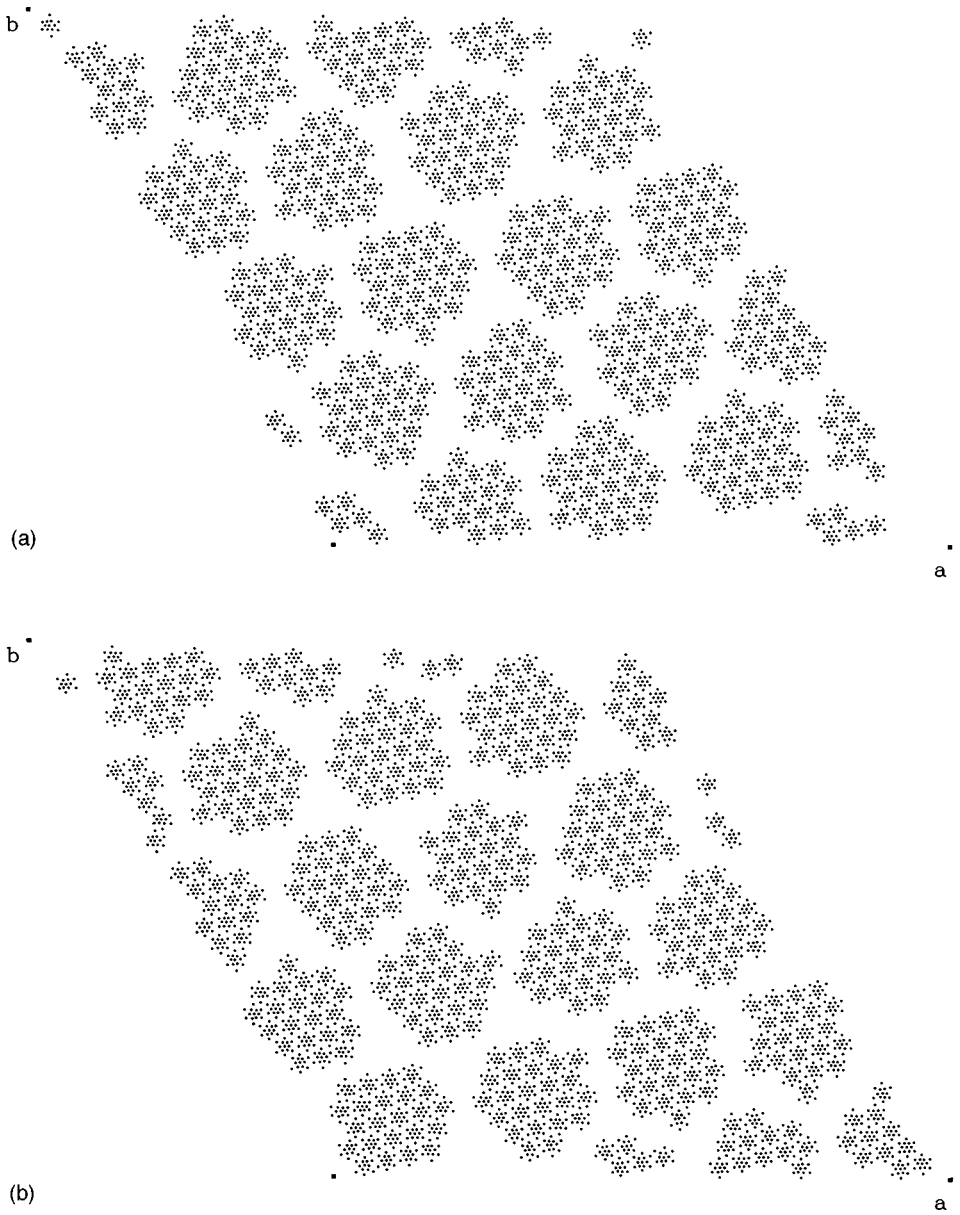

FIG. 8. (a) Ta atoms in the layer $z=0$ in a region of 100×100 unit cells. Only atoms belonging to complete clusters are plotted as dots. The regions with domain-wall-like structure are left blank. The modulation in x,y direction for the Ta atoms is exaggerated five times. The origin $(t_1,t_2)=(0,0)$ is the lower left point. (b) The same as (a) for the Ta atoms in the layer $z=\frac{1}{3}$. (c) Ta atoms in the layer $z=0$. An enlargement of (a) is shown, now with the atoms in the domain walls plotted as heavy dots.

of corner-sharing triangles. This result is different from the model proposed by Yamamoto,[25] who proposed the honeycomb lattice as domain structure. However, our result is in excellent agreement with the theory of Nakanishi and Shiba,[17] who indeed found a pattern of corner-sharing hexagons as the domain structure of the NC phase (Fig. 3 in Ref. 17).

The relation between the structures of different layers is determined by the centering translations $(E|0,0,\frac{1}{3},\pm\frac{2}{3},\pm\frac{1}{3})$, or equivalently by the commensurate components of the modulation wave vectors. The phase shifts of the modulation in neighboring layers therefore are $\pm(-\frac{1}{3},\frac{1}{3})$. The effect in the structure is that the centers of the domains in neighboring layers are shifted such that the centers of the domains in one layer are on top of the centers of one half of the triangular regions forming the domain walls (Fig. 8). The domains thus form a pattern similar to a hexagonal close packed lattice.

C. Correlation between tantalum and sulfur modulations

The modulation of the S atom is much smaller than that of Ta. It has contributions in all three directions, but the largest amplitudes are along **c** (Table V). The u_z modulation of S ($\frac{2}{3}$, $\frac{1}{3}$, 0.086) at the position ($\frac{2}{3}$, $\frac{1}{3}$, 0.086) is drawn as a function of (t_1,t_2) in Fig. 10. The threefold site symmetry of the S atom is clearly visible. The z modulation can be characterized by large plateaus with positive displacement ($u_z=0.106$ Å) and slightly smaller plateaus with negative displacement ($u_z=-0.124$ Å). The boundaries between the positive and negative regions are rather sharp, and a block wave is a reasonable approximation for this function.

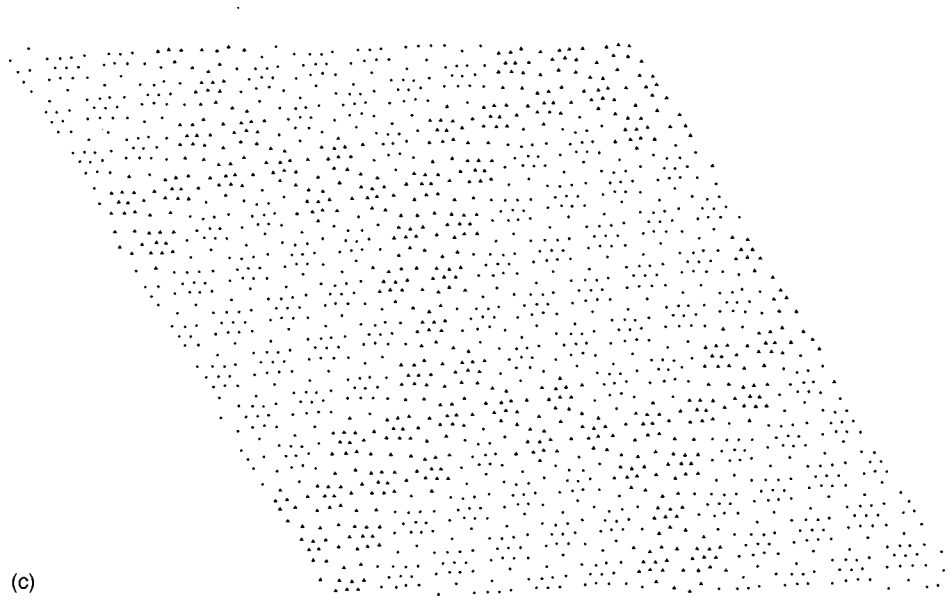

FIG. 8. (*Continued*).

The correlation between these displacements of S and Ta can be obtained by comparing t plots of the z displacement of S with t plots of Ta-Ta interatomic distances. For example, the point $t_1=t_2=0.0$ corresponds to a minimum in the distance between Ta (0,0,0) and Ta (1,0,0), while S ($\frac{2}{3}$, $\frac{1}{3}$, 0.086) directly above this pair of Ta atoms exhibits a maximum displacement away from both Ta atoms (Figs. 3 and 10). Similarly, Figs. 3 and 10 show that at a point (t_1,t_2) where the distance between neighboring Ta atoms is a maximum [e.g., $(t_1,t_2)=(0.245,-0.068)$], the u_z modulation of the S atom is a minimum and negative. In the basic structure, S ($\frac{2}{3}$, $\frac{1}{3}$, 0.086) is directly above the triangle formed by Ta

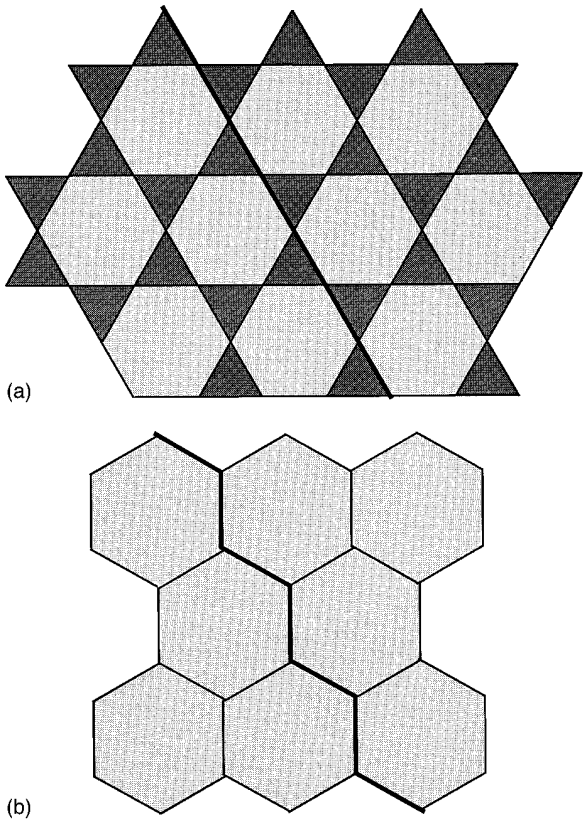

FIG. 9. Two possibilities for a structure consisting of domains with hexagonal shape. (a) is found for straight boundaries for the jump of the phase of the order parameter, and corresponds to a structure of corner sharing hexagonal domains, separated by regions of domain-wall-type structure in the form of a lattice of triangles. (b) is realized with zig-zag phase boundaries, resulting in a honeycomb lattice of hexagons.

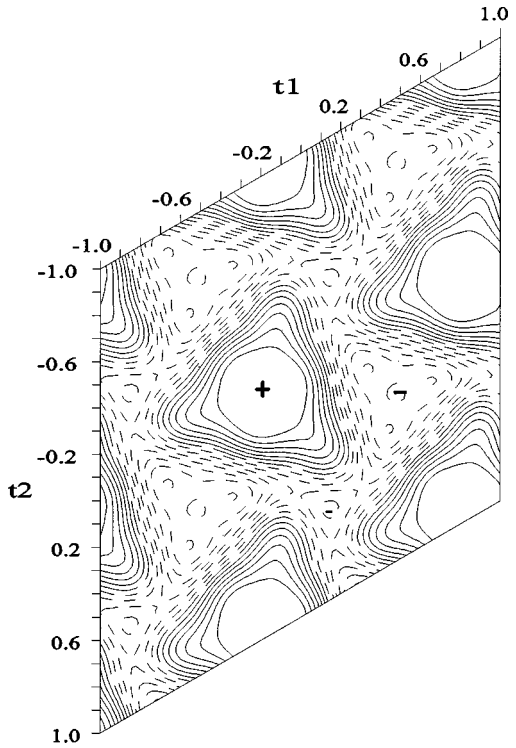

FIG. 10. Modulation in the z direction of the S atom on position ($\frac{2}{3}$, $\frac{1}{3}$, 0.086). Contours are shown at intervals of 0.0177 Å. The maximum displacement, indicated by a plus sign, is 0.106 Å and the minimum displacement, indicated by a large minus sign, is -0.124 Å.

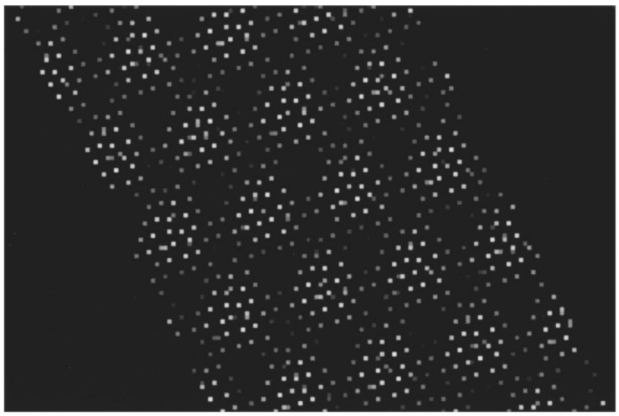

FIG. 11. Modulation in the z direction of the S atom. Increasing brightness means a larger displacement towards the positive z directions. Only atoms with $u_z > 0.1$ Å are shown.

(0,0,0), Ta (1,0,0), and Ta (1,1,0) (Fig. 7). Extending the comparison of t plots, then shows that the u_z modulation of the S has a maximum for those phase values where the distances between the three underlying Ta atoms are a minimum and vice versa (Figs. 3, 4, 5, and 10). It is thus found that there is a strong correlation between the modulations of Ta and S, such that sulfur atoms are pushed out of the layer when the coordinating tantalum atoms move towards each other, and the other way around. Further analysis shows this to be a general property of the modulation, implying that all sulfur atoms above a 13 cluster move outwards, and that sulfur atoms between 13 clusters and within the domain walls move towards the center of the layer. This result is in accordance with a similar finding for the commensurate superstructure.[7]

The hcp stacking of layers is now explained by the sulfur modulation. Above one domain, most sulfur atoms move away from the center-plane of that layer, i.e., they move towards the next layer. At these positions, the next layer has its triangular domain-wall region, where there are many long Ta-Ta distances, and most sulfur atoms will have moved towards the center plane of this layer. The sulfur displacements in neighboring layers thus are in anticorrelation, such that the variation in sulfur-to-sulfur distances across the Van der Waals gap is a minimum, and a maximum packing density can be reached.

STM images the surface, which for TaS_2 consists of a plane of sulfur atoms. STM on $1T$-TaS_2 exhibited a pattern compatible with a domain structure of the NC phase.[23] In the present investigation, it was shown that the domain structure is reflected in the z modulation of the S atoms. Positive displacements were found for the underlying Ta atoms belonging to 13 clusters, while negative displacements were found for underlying Ta atoms in the domain-wall region. Accordingly, the z displacement of sulfur directly correlates with domains and domain walls. A simulated STM image was now generated, by plotting the sulfur atoms as dots with a brightness proportional to the z displacement (Fig. 11). A striking similarity is observed with the STM image of the NC of $1T$-TaS_2 obtained by Thompson *et al.* (Figure 10(c) in Ref. 23), and it is concluded that the result of the present structure determination is in accordance with STM.

VI. CONCLUSIONS

The modulated structure has been determined of $1T$-TaS_2 in its nearly commensurate state. A large number of harmonics for the modulation functions were included in the refinements, and the result indicated that the shapes of the modulation functions can be approximated by a block wave. In physical space this corresponds to a domain structure, where the structure within the domains is that of the commensurate $\sqrt{13}a \times \sqrt{13}a$ superstructure. Maybe the most salient feature is that we have been able to determine the shapes of the domains from a crystallographic analysis of the intensities of Bragg reflections in x-ray scattering. It was found that the domains have a distorted hexagonal shape. The domain walls are not regions of constant width, but instead they form a pattern of corner-sharing triangles, as left over by the corner-sharing hexagonal domains. This finding is in complete accordance with the theoretical prediction by Nakanishi and Shiba[17] but deviates from previous x-ray scattering work.[25]

From the z displacements of the sulphur atoms a simulated STM picture was calculated that showed a striking similarity with the experimental STM image published in Ref. 23. It is thus concluded that the result of STM and x-ray diffraction are in accordance with each other.

*Electronic address: smash@uni-bayreuth.de

[1] F. Jellinek, J. Less-Common Met. **4**, 9 (1962).
[2] J. van Landuyt, G. van Tendeloo, and S. Amelinckx, Phys. Status Solidi A **26**, 197 (1974); **26**, 585 (1974); **36**, 767 (1976).
[3] J. A. Wilson and A. D. Yoffe, Adv. Phys. **18**, 193 (1969).
[4] A. H. Thompson, F. R. Gamble, and J. F. Revelli, Solid State Commun. **9**, 981 (1971).
[5] C. B. Scruby and P. M. Williams, Philos. Mag. **31**, 255 (1975).
[6] J. A. Wilson, F. J. Di Salvo, and S. Mahajan, Adv. Phys. **24**, 117 (1975).
[7] R. Brouwer, Ph.D. thesis, University of Groningen, The Netherlands, 1978.
[8] K. K. Fung, J. W. Steeds, and J. A. Eades, Physics B **99**, 47 (1980).
[9] S. Tanda, T. Sabonge, T. Tani, and S. Tanaka, J. Phys. Soc. Jpn. **53**, 476 (1984).
[10] K. Nakanishi and H. Shiba, J. Phys. Soc. Jpn. **53**, 1103 (1984).
[11] O. Sezerman, A. M. Thomson, and M. H. Jericho, Solid State Commun. **36**, 737 (1980).
[12] T. Haga, Y. Abe, and Y. Okwamoto, Phys. Rev. Lett. **51**, 678 (1983).
[13] A. Suzuki, R. Yamamoto, M. Donya, H. Mizubayashi, S. Okuda, K. Endo, and S. Gonda, Solid State Commun. **49**, 1173 (1984).
[14] R. L. Whithers and J. W. Steeds, J. Phys. C **20**, 4019 (1987).
[15] Y. Yamada and H. Takatera, Solid State Commun. **21**, 41 (1977).
[16] K. Nakanishi, H. Takatera, Y. Yamada, and H. Shiba, J. Phys. Soc. Jpn. **43**, 1509 (1977).
[17] K. Nakanishi and H. Shiba, J. Phys. Soc. Jpn. **43**, 1839 (1977).
[18] X. L. Wu and C. M. Lieber, Science **243**, 1703 (1990).
[19] X. L. Wu and C. M. Lieber, Phys. Rev. Lett. **64**, 1150 (1990).
[20] B. Burk, R. E. Thomson, A. Zettle, and J. Clarke, Phys. Rev. Lett. **66**, 3040 (1991).

[21] R. V. Coleman, W. W. McNairy, and C. G. Slough, Phys. Rev. B **45**, 1428 (1992).
[22] H. Ohta, T. Takasa, Y. Komiya, H. Miyamoto, S. Mishima, T. Okada, and K. Nomura, Phys. Status Solidi B **169**, 313 (1992).
[23] R. E. Thomson, B. Burk, A. Zetll, and J. Clarke, Phys. Rev. B **49**, 16 899 (1994).
[24] R. Brouwer and F. Jellinek, Mater. Res. Bull. **9**, 827 (1974).
[25] A. Yamamoto, Phys. Rev. B **27**, 7823 (1983).
[26] A. Janner, T. Janssen, and P. M. de Wolf, Acta Crystallogr. Sect. A **39**, 658 (1983).
[27] S. van Smaalen, Crystallogr. Rev. **4**, 79 (1995).
[28] V. Petricek, Crystallographic Computing System JANA, Version October 1994.
[29] W. L. McMillan, Phys. Rev. B **14**, 1496 (1976).